Role of elastic bending stress on magnetism of a manganite thin film studied by polarized neutron reflectometry

Surendra Singh, M. R. Fitzsimmons, T. Lookman, H. Jeen, A. Biswas, M. A. Roldan, and M. Varela

The exclusive role of applied stress on magnetism of a manganite film

Surendra Singh,[1,2] M. R. Fitzsimmons,[1] T. Lookman,[1] H. Jeen,[3,*] A. Biswas,[3] M. A. Roldan[4] and

M. Varela[5]

[1]Los Alamos National Laboratory, Los Alamos, NM 87545, USA

[2] Solid State Physics Division, Bhabha Atomic Research Center, Mumbai 400085, India

[3]Department of Physics, University of Florida, Gainesville, FL 32611, USA

[4]University Complutense, Madrid 28040, Spain

[5]Oak Ridge National Laboratory, Oak Ridge TN 37831 USA

Abstract: We measured the magnetization depth profile of a $(La_{1-x}Pr_x)_{1-y}Ca_yMnO_3$ (x =0.60±0.04, y= 0.20±0.03) film using polarized neutron reflectometry as functions of applied elastic bending stress and temperature. We found unequivocal and till now elusive direct evidence that the exclusive application of compressive (tensile) bending stress along the magnetic easy axis increases (decreases) the saturation magnetization of the film. Further, we obtained a coupling coefficient relating strain to the depth dependent saturation magnetization.

[*]Presently at Oak Ridge National Laboratory, Oak Ridge TN 37831 USA.

Collective interactions between charge, spin, orbital and lattice order[1,2,3,4] can lead to complex behavior in doped manganites such as colossal magnetoresistance (CMR) and metal insulator transitions (MIT) that may result from coexistence of ferromagnetic, metallic and insulating phases.[5,6,7,8,9] These interactions can be greatly influenced by the environment, e.g., by magnetic field,[8] light,[10] stress,[4,11,12,13,14,15,16,17] disorder,[16] etc. In bulk $La_{0.65}Ca_{0.35}MnO_3$ (LCMO), application of hydrostatic pressure increases the ferromagnetic Curie temperature, T_c,[18] thus, compressive strain in bulk LCMO strengthens the ferromagnetic phase.

Theory suggests that phase coexistence in $(La_{1-x}Pr_x)_{1-y}Ca_yMnO_3$ (LPCMO) films can be tuned by strain.[4] In one report Millis *et al.*,[15] found a shift of T_c of a CMR film could be 10% for 1% biaxial strain. A second theoretical study[19] reported that reduction of manganite film thickness and/or increased tensile (compressive) stress decreased (increased) T_c, thus, weakening (strengthening) the ferromagnetic phase. However, Yuan[20] argues that tensile strain should increase the Mn-O-Mn bond angle and strengthen the ferromagnetic phase.

Phase coexistence in manganites[5,6,7,8,9] has been attributed to the influence of quenched disorder, e.g., chemical or strain non-uniformity, in the vicinity of a first-order transition,[16] as well as to long-range strain mediated interactions.[4,17] For example, disorder can lead to pinning of phase boundaries[16] thereby inhibiting transformation. Alternatively, long range strain may influence the fractions of metallic vs. insulating phases (perhaps affecting ferromagnetic order).

Experiments measuring the response of magnetism to stress in manganite films have provided a decidedly mixed picture. Namely, some studies[12,21] report compressive strain strengthens the ferromagnetic phase [meaning that one or more of T_c, saturation (M_s), or remanent (M_r) magnetization, or the metal-insulator transition temperature (T_{MI})(T_{MI} is indirectly related at best to magnetism), increase], or that tensile strain weakens the ferromagnetic

phase.[13,21] However, other studies[22,23] report tensile strain produces exactly the opposite behavior and in another study[13] compressive strain had negligible effect on magnetism. These studies claim to have explored the influence of strain on magnetism by comparing different films grown under different conditions, on different substrates or with different chemical compositions. However, none of these experiments examined the exclusive role of stress on magnetic properties, and the different conclusions have led to possible contradictions in the effect of strain on the magnetism of manganites.

In order to clarify the influence of strain on the electronic and magnetic properties of complex oxides, some studies have used structural phase transformation[23] or the piezoelectric property[24] of a substrate, or mechanical jigs[25] to apply stress to films. The first two techniques are suitable only for films that can be epitaxially grown on particular substrates. (Mechanical jigs can apply stress to a wide range of samples.) Even with the intention to clarify the role of stress on magnetism, the first two studies (Refs. [23] and [24]) still yielded contradictory results. In one case an *increase* of M_s was correlated with *expansion* of the in-plane area change of between 0.1 and 0.2%.[23] In the second case, *increases* of M_r and T_c were correlated with *decreases* of tensile strain.[24] If the applied stress produced strain of 0.1 to 0.2% as suggested for either case, then the strain was possibly not elastic. The elastic strain of a manganite film is of order 0.06%.[26] Thus, a concern is whether the dislocations formed during yielding may have been a source of quenched disorder that affected phase separation and the electronic/magnetic properties of the films differently.

Here, we report measurements of the saturation magnetization depth profile of a $(La_{1-x}Pr_x)_{1-y}Ca_yMnO_3$ (x =0.60±0.04, y= 0.20±0.03) single crystal film as a function of systematically applied *compressive* and *tensile* elastic bending stress. Because our study is one of a single

sample being stressed well within the elastic regime, we have unequivocally determined the exclusive role of stress on the saturation magnetization.

A 1 cm by 1 cm by 25-nm-thick single crystal film with the nominal composition of $(La_{1-x}Pr_x)_{1-y}Ca_yMnO_3$ (x = 0.60, y = 0.33) was epitaxially grown on a (110) $NdGaO_3$ (NGO) substrate in the step-flow-growth-mode using pulsed KrF laser (248 nm) deposition (PLD).[27] During growth, the substrate temperature was 780°C, O_2 partial pressure was 130 mTorr, laser fluence was 0.5 J/cm^2, and the repetition rate of the pulsed laser was 5 Hz. The thickness of the substrate was 0.25 mm.

Bending stress was applied to the film using a four point bending jig (Fig. 1(a)). A four point jig applies stress uniformly over the lateral dimensions of a large sample.[28] Furthermore, since the film thickness is small compared to the substrate thickness, the stress is uniform across the film's out-of-plane direction (the plane of zero stress lies halfway inside the substrate)—this attribute distinguishes our approach from those of Refs. [23] and [24] which utilized techniques that produced strain gradients normal to the film's surface. Thus, our experiment is not sensitive to flexomagnetism as discussed in Ref. [29]. Tensile ($\varepsilon > 0$) and compressive ($\varepsilon < 0$) strain of the thin film can be realized by placing the film in contact with or opposite to the inner supports of the jig, respectively (Fig. 1(b)). The innovation of our experiment is the design of the four point bending jig that enables simultaneous measurement of the resistance (with current parallel to the sample's surface) and the neutron reflectivity of the sample, as functions of temperature, applied magnetic field and stress, from which the magnetic depth profile as functions of these parameters can be obtained. The jig and experimental protocol are likely to have impact on a broad range of important materials, including piezeomagnetic and multiferroic materials.

Bending stress was applied parallel to the magnetic easy axis of the sample, which is parallel to [1$\bar{1}$0] NGO.[30] The sample was cooled or warmed in the 6 kOe field (applied along the easy axis) at a rate of 0.4 K/min. The 6 kOe field is an order of magnitude larger than the field required to saturate the magnetization.[30] Transport measurements for the sample with ε = ± 0.011% and ε = 0% (without applied stress) are shown in Fig. 1(c). The bending strain of the film was measured using:[31] $\varepsilon = \frac{t_s}{R}$, where t_s and R are the thickness of substrate and the radius of curvature of film, respectively. The radius of curvature of the sample was measured with a laser.[32]

To independently examine the chemical depth profile, we measured a small portion of our sample with electron energy-loss spectroscopy (EELS).[33] While the average composition of the film was $(La_{1-x}Pr_x)_{1-y}Ca_yMnO_3$ (x = 0.60±0.04, y = 0.20±0.03), we observed three chemically distinct regions (surface, film-bulk and film-substrate)[33] similar to those observed in our earlier study of another similarly prepared sample.[30] The EELS data suggest a variation in the Mn^{4+}:Mn^{3+} ratio along the depth of the film, particularly near the film-substrate interface.

Polarized neutron reflectivity (PNR) measurements of the sample were obtained using the Asterix spectrometer at the Los Alamos Neutron Science Center.[34] In PNR the intensity of the specularly reflected neutron beam is compared to the intensity of the incident beam as a function of wave vector transfer, Q (= $4\pi sin\theta/\lambda$, where, θ is angle of incidence and λ is neutron wavelength), and neutron beam polarization. The specular reflectivity, R, is determined by the neutron scattering length density (SLD) depth profile, $\rho(z)$, averaged over the lateral dimensions of the sample. $\rho(z)$ consists of nuclear and magnetic SLDs such that $\rho^{\pm}(z) = \rho_n(z) \pm CM(z)$, where $C = 2.853\times10^{-9}$ Å^{-2}(kA/m)$^{-1}$ and $M(z)$ is the magnetization (a moment density obtained in kA/m) depth profile.[34] The +(-) sign denotes neutron beam polarization parallel (opposite) to the

applied field and corresponds to reflectivities, $R^{\pm}(Q)$. Thus, by measuring $R^{+}(Q)$ and $R^{-}(Q)$, $\rho_n(z)$ and $M(z)$ can be obtained separately. The reflectivity datawere normalized to the Fresnel reflectivity[34] ($R_F = \frac{16\pi^2}{Q^4}$) and are shown in Figs. 2 and 3.

Before bending the sample, we measured the x-ray reflectivity (XRR) of the sample at room temperature and its reflectivity with polarized neutron beams at 200 K and 40 K in a 6 kOe strong field. The XRR and PNR data were analyzed using the method of Parratt.[33,35] Motivated by EELS, the chemical depth profile of the sample was represented by three chemically distinct regions. Discussion of the chemically distinct regions and their magnetizations in the unstrained state can be found in Ref. [30]. The model was fitted to the XRR data to obtain the thicknesses of each region and the length scale over which the chemical profile changed (from region to region). The chemical model of the sample was then used in a second model to obtain the magnetization depth profile from the PNR data as the sample was bent.

In order to study the coupling between strain and magnetism, we carried out PNR measurements as a function of applied stress at constant temperature, T. We also performed measurements for constant ratios of temperature to transition temperature ($T/T_{IM} = T/T_{MI} = 0.93$) while cooling and warming across the MIT's. T_{IM} (insulator to metal transition) and T_{MI} (metal to insulator transition) temperatures are defined as temperatures at which the resistance changed by 95% of its maximum value during the cooling and warming cycles, respectively. We performed measurements at constant T (open circles Fig. 1(c)) and T-ratios (open triangles in Fig. 1(c)) (temperatures normalized by the metal-insulator transition temperatures) in case stress changed T_c.

Fig. 2(c) and (d) show the $M(z)$ profile of the sample taken for constant T (78 K) and T/T_{IM} in Figs. 2(a) and (b) respectively. The $M(z)$ profiles were obtained from the PNR data by fitting

a model in which only the saturation magnetization of each region was varied. Similarly while warming the sample, we measured PNR data for constant T (89 K) and constant T/T_{MI}, and these data are shown in Fig. 3. The analysis shows compelling evidence that compressive strain increases the average magnetization while tensile strain suppresses the average magnetization. The trends are realized regardless of whether the measurements were made for constant temperature or constant ratio of temperature to metal-insulator (insulator-metal) transition temperature. Furthermore, the trends are the same regardless of the chemical composition of the region (e.g., as shown by regions I, II and III in the inset of Fig. 2(c)).

From the PNR data the magnetization was obtained in kA/m. From these data and the number density of Mn in bulk LCMO,[36] the magnetization can be expressed in terms of moment per Mn atom (right hand side of Figs. 2 and 3). However, we do not imply the moment resides on the Mn site. Indeed, polarized neutron diffraction has determined for the case of $La_{1.2}Sr_{1.8}Mn_2O_7$ that some moment resides on oxygen.[37]

Upon application of small tensile (compressive) bending stress (i.e. $|\varepsilon|$ ~0.011%) we observed a shift in T_{MI} (or T_{IM}) of about 3 K to lower (higher) temperature (Fig. 1(c)). The shift of the MIT to higher temperature and consequential reduction in resistance at fixed temperature upon application of compressive stress is consistent with an earlier study.[25] We also observed a ~ 20% increase of M_s for compressive stress, and a ~20% decrease of M_s for tensile stress at T= 78 K (Fig. 2 (c)). The LPCMO film without applied stress exhibited a paramagnetic to ferromagnetic transition temperature of T_c ~ 130 K.[27,30,33] If the large change of M_s were attributed to a change of T_c, then T_c would have changed by ~ 100 K to account for the change of M_s (inferred from a fit of the Brillouin function to the temperature dependence of M_s as measured with SQUID magnetometry for the LPCMO film without applied stress[33]). Such a shift

is much larger than that suggested by Millis *et al.*[15] Further, such a change of T_c would be much larger than the 6 K change observed for a more highly strained (0.06%) $La_{0.7}Sr_{0.3}MnO_3$ film.[24]

An alternative explanation is to suppose the M_s and ε are coupled. We considered a strain contribution to the usual free energy of a magnetic system including piezomagnetic and magnetoelastic contributions by: $F_c = \gamma\varepsilon M_\varepsilon^2 + \frac{A}{2}\varepsilon^2$, where γ, ε, A and M_ε are the coupling coefficient [units of N/A^2], strain, Young's modulus [units of N/m^2] and change of magnetization due to strain, respectively. Assuming our measurements are taken for a system in equilibrium; we obtain a relation for the coupling constant by minimizing the F_c with respect to strain, yielding: $M_\varepsilon^2 = -\frac{A}{\gamma}\varepsilon$. The total magnetization on application of strain is given by: $M^2 = M_0^2 + $

$M_\varepsilon^2 = M_0^2 - \frac{A}{\gamma}\varepsilon$, where M_0 is the saturation magnetization of the system at $\varepsilon = 0$. Thus, from the slope of M^2 vs. ε, (Fig. 4) $-A/\gamma$ is obtained. Using nanoindentation,[38] we measured Young's modulus, A, of our film to be $A = 200$ GPa.

The M^2 vs. ε curve for different regions at constant T and constant $T/T_{MI(IM)}$ ratios (Fig. 2 and Fig. 3) are plotted in Figs. 4(a-f). The slopes of these curves are negative; indicating that compressive strain favors the ferromagnetic phase as evidenced by an increase of saturation magnetization. The γ's for different regions are plotted in Fig. 4(g). γ is smallest for LPCMO film-bulk (region II) compared to the surface and interface regions (regions I and III). A small value of coupling coefficient, γ, suggests a strong coupling of magnetism and strain in the sense that a small applied bending stress will produce a large change of magnetization. Thus, we find the coupling between strain and magnetism to be most pronounced for the stoichiometric composition of $(La_{1-x}Pr_x)_{1-y}Ca_yMnO_3$ (x =0.60±0.04, y= 0.20±0.03) than for the surface or film-substrate interface.

For the film bulk (region II), we observed a coupling coefficient ranging from γ = 0.00029(1) N/A^2 at T= 78 and 89 K (for the cooling and warming cycles, respectively) to γ =0.00057(1) N/A^2 for constant T-ratio. The coupling coefficients for surface and interface regions (region I and III) are much larger ranging from 0.002(1) to 0.004(1) for the same temperatures and T-ratio. The coupling coefficients of regions I and III are approximately a factor of seven larger than that of region II. We attribute this difference to the difference between the chemistry (including Mn valence) and its influence on magnetization. The square of the ratio of magnetization of the film bulk to that of the surface and interface regions is about nine.

In summary, we have measured the saturation magnetization depth profiles across an LPCMO film as a function of the exclusive application of elastic stress. We found the strongest coupling between strain and magnetization for the bulk film with the composition of $(La_{1-x}Pr_x)_{1-y}Ca_yMnO_3$ (x =0.60±0.04, y= 0.20±0.03). The coupling is weaker for the film's surface and film-substrate interface. The film-substrate interface is oxygen and Mn^{4+} rich. In contrast to the behavior of magnetic transition elements (where compressive stress promotes d-band hybridization, thus lowering magnetization[39]), we find that compressive stress in our LPCMO film strengthens the ferromagnetic phase as evidenced by increases of the average saturation magnetization (over a broad range of stoichiometry), whereas tensile stress decreases the average saturation magnetization. Our results clarify a conflicting picture of the influence of stress on the magnetic properties of manganite films and suggests that long range strain plays an important role across the MIT since applied stress changed both the MIT temperature (~ 3K) and the magnetization (~ 20%) of the film.
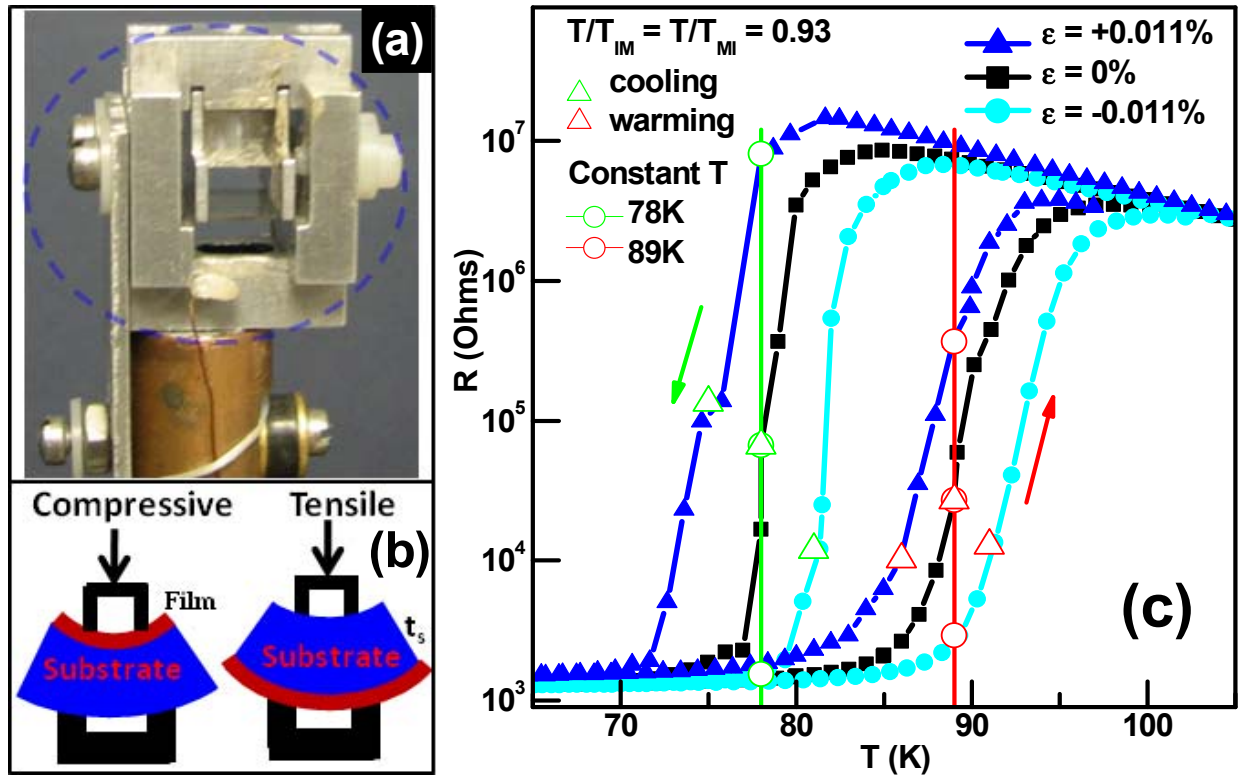
Fig. 1: End-view image of the four point jig (circled) mounted on a cryostat (a) and side-view schematic representation of applied bending stress (b). (c): Transport measurements of the film at different applied bending stress/strain, tensile (▲), compressive (●) and no strain (■). Open circles and open triangles represents constant T and constant T-ratio ($T/T_{IM} = T/T_{MI} = 0.93$) at which we simultaneously measured the neutron reflectivities.
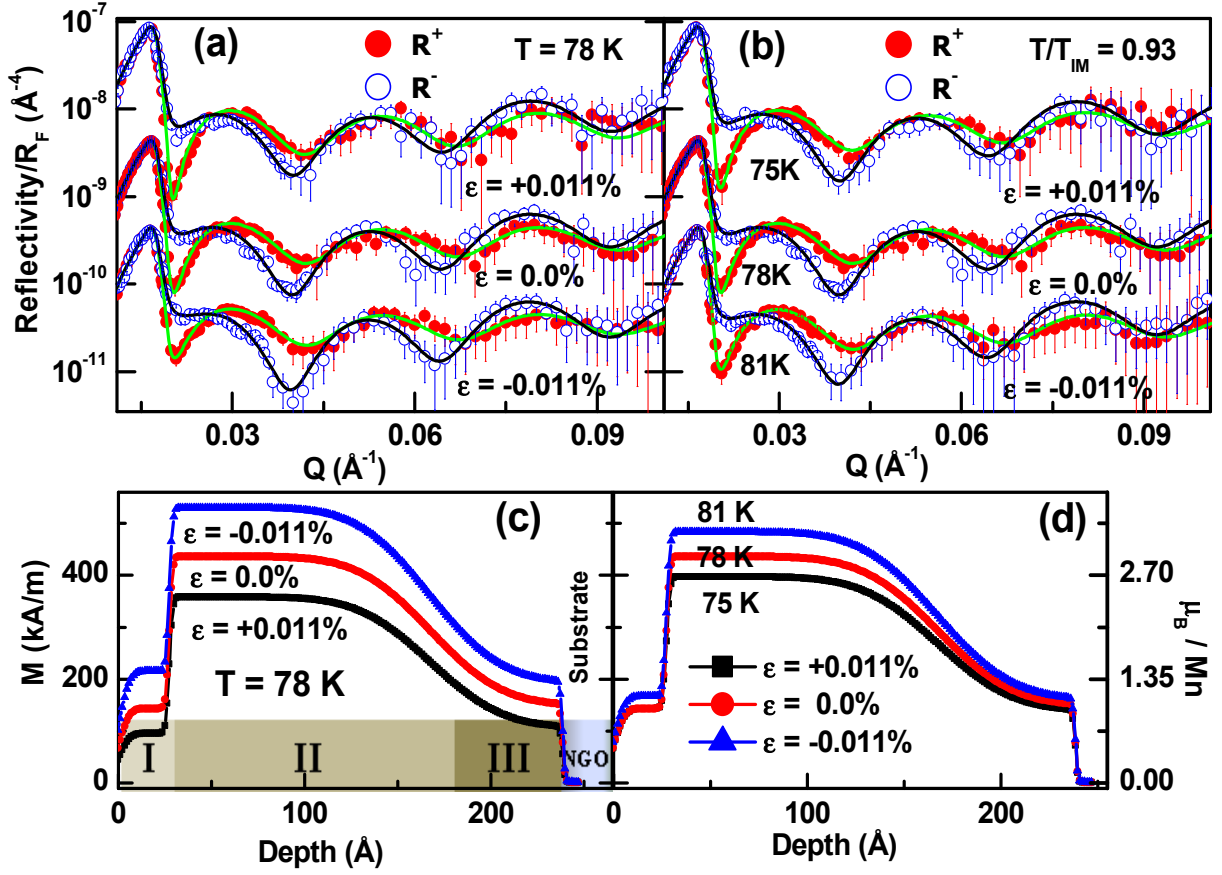
Fig. 2: PNR measurements from LPCMO film for different applied strain at constant temperature (a) and constant T/T_{IM} (b) while cooling. Reflectivity data at different applied stress/strain are shifted by a factor of 5 for the sake of clarity. (c) and (d) show the magnetization (M) depth profile corresponding to (a) and (b) respectively.
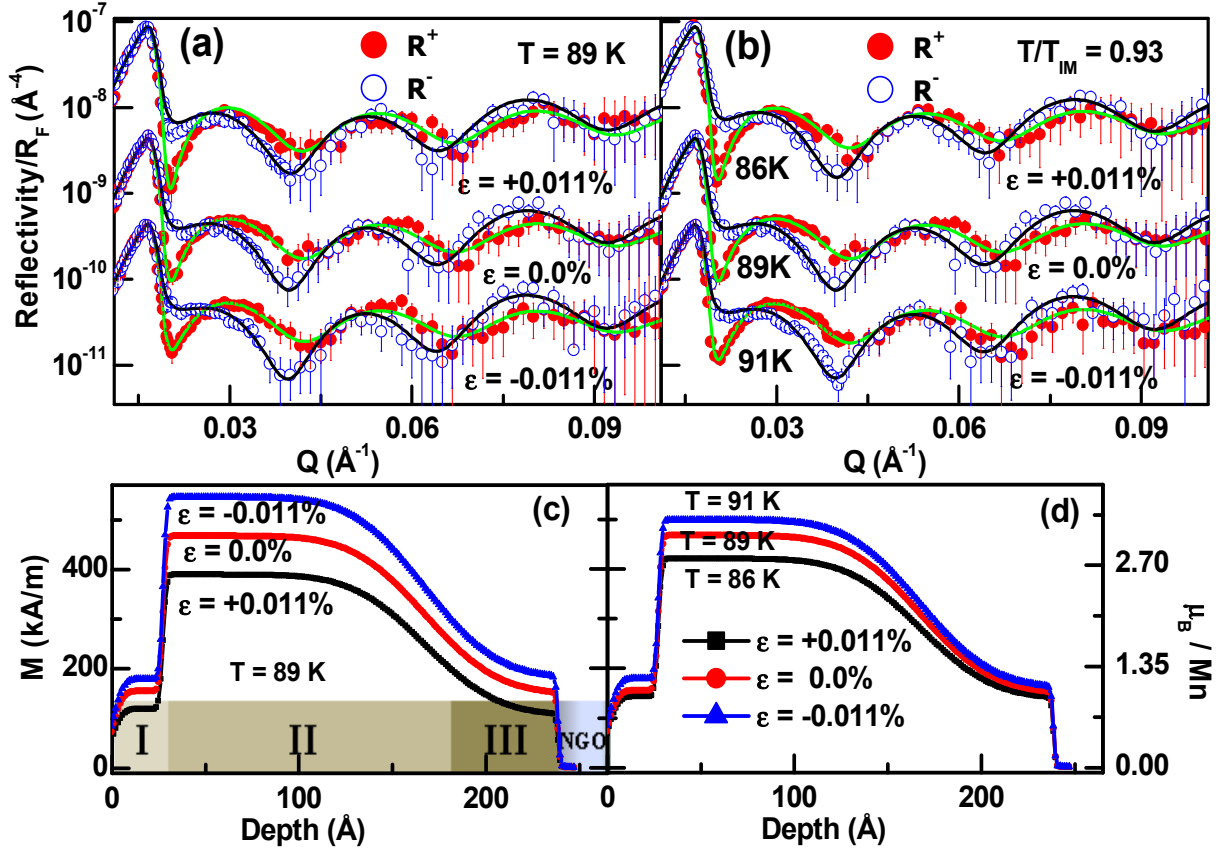
Fig. 3: PNR measurements from LPCMO film for different applied strain at constant temperature (a) and constant T/T_{MI} (b) while warming. Reflectivity data at different applied stress/strain are shifted by a factor of 5 for the sake of clarity. (c) and (d) show the magnetization depth profile corresponding to (a) and (b) respectively.
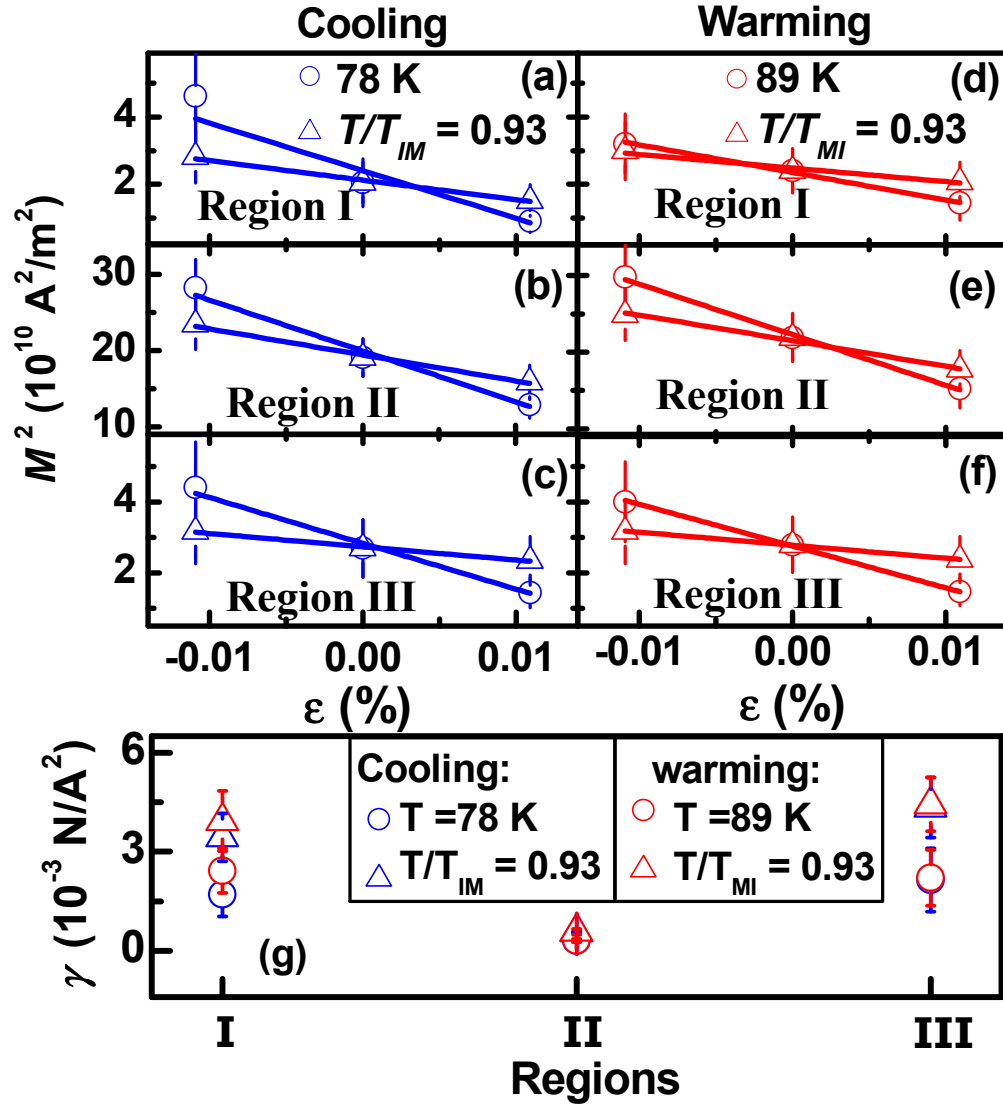
Fig. 4: (a)-(f): Variation of magnetization as a function of strain at different temperatures of cooling (left panel) and warming (right panel) for different regions of LPCMO film. The lines are the best fits obtained from linear regression. (g): Coupling coefficient, γ, for different region at different temperatures.

[1] A. J. Millis, Nature **392**, 147 (1998).

[2] Y. Tokura and N. Nagaosa, Science, **288**, 462 (2000).

[3] N. D. Mathur and P. B. Littlewood, Physics Today*56*, 25 (2003).

[4] K. H. Ahn, T. Lookman, and A. R. Bishop, Nature **428**, 401 (2004).

[5] E. Dagotto, *Nanoscale Phase Separation in Manganites* (Springer-Verlag, Heidelberg, 2002).

[6] M. B. Salamon and M. Jaime, Rev. Mod. Phys., **73**, 583 (2001).

[7] S. Jin, et al., Science **264**, 413 (1994).

[8] M. Ueharaet al., Nature**399**, 560 (1999).

[9] M. Bibes et al., Phys. Rev. Lett. **87**, 067210 (2001).

[10] K. Miyano et al., Phys. Rev. Lett. **78**, 4257 (1997).

[11] T. Z. Ward et al., Nat. Phys.**5**, 885 (2009).

[12] X.J. Chen et al. Phys. Rev. B **65**, 174402 (2002).

[13] D.Gillaspie et al., J Appl. Phys., **99**, 08S901 (2006).

[14] F. H. Zhang et al., Appl. Phys. Lett.**96**, 62507, (2010).

[15] A. J. Millis, T. Darling and A. Migliori, J. Appl. Phys.**83**, 1588 (1998).

[16] E. Dagotto, Science**309**, 257-262 (2005).

[17] A. Sartbaeva et al., Phys. Rev. Lett. **97**, 065501 (2006).

[18] B. Lorenz et al., Phys. Rev. B **63**, 144405 (2001).

[19] C.A. Perroni et al., Phys. Rev. B **68**, 224424 (2003).

[20] Q. Yuan, Phys. Rev. B **70**, 066401 (2004).

[21] X. J. Chen et al., Phys. Rev. B**72**, 104403 (2005).

[22] J. Zhang et al., Phys. Rev. B **64**, 184404 (2001).

[23] M. K. Lee et al., Appl. Phys. Lett.**77,** 3547 (2000).

[24] C. Thiele et al., Appl. Phys. Lett. **87,**262502 (2005).

[25] J. Tosado, T. Dhakal and A. Biswas, J. Phys.: Condens. Matter **21**, 192203 (2009).

[26] Using the yield strength of 120 to 300 MPa for $SrTiO_3$ [P. Gumbsch et al., Phys. Rev. Lett. **87**, 085505 (2001)] and Young's modulus of 200 GPa measured for our LPCMO film, the maximum elastic strain of our LPCMO film is of order 0.06%.

[27] H. Jeen and A. Biswas, Phys. Rev. B **83**, 064408 (2011).

[28] B. Hammant, Composites **2**, 246 (1971).

[29] P. Lukashev and R. F. Sabirianov, Phys. Rev. B **82**, 094417 (2010).

[30] S. Singh, et al., Phys. Rev. Lett. **108**, 077207(2012).

[31] A. Misra and M. Nastasi, *Engineering Thin Films and Nanostructures with Ion Beams* (CRC Press, 2005), Chap. 7, pp. 319.

[32] Y. T. Im et al., J. Mech. Sci. Tech., **18**, 12 (2004).

[33] See supplementary material for EELS data, XRR (room temperature) and PNR data at 200K and 40K.

[34] M. R. Fitzsimmons and C. Majkrzak, *Modern Techniques for Characterizing Magnetic Materials* (Springer, New York, 2005), Chap. 3, pp. 107–155.

[35] L. G. Parratt, Phys. Rev. **95**, 359 (1954).

[36] G.H.A. Therese and P.V. Kamath, Chem. Mater. **10**, 3364 (1998).

[37] D.N. Argyriou et al., Phys. Rev. B **65** 214431 (2002).

[38] W. C. Oliver and G. M. Pharr, J. Mater. Res. **7**, 1564 (1992).

[39] V. Iota, et al., Appl. Phys. Lett. **90**, 042505 (2007).